The stress-regulated protein p8 mediates cannabinoid-induced apoptosis of tumor cells

Arkaitz Carracedo,[1] Mar Lorente,[1] Ainara Egia,[1] Cristina Blázquez,[1] Stephane García,[2] Valentin Giroux,[2] Cedric Malicet,[2] Raquel Villuendas,[3] Meritxell Gironella,[2] Luis González-Feria,[4] Miguel Ángel Piris,[3] Juan L. Iovanna,[2] Manuel Guzmán,[1] and Guillermo Velasco[1,*]

[1] Department of Biochemistry and Molecular Biology I, School of Biology, Complutense University, 28040 Madrid, Spain
[2] U624 INSERM, Campus de Luminy, 13288 Marseille Cedex 9, Marseille, France
[3] Centro Nacional de Investigaciones Oncológicas, Instituto de Salud Carlos III, 28029 Madrid, Spain
[4] Department of Neurosurgery, University Hospital, 38320 Tenerife, Spain
*Correspondence: gvd@bbm1.ucm.es

Summary

One of the most exciting areas of current research in the cannabinoid field is the study of the potential application of these compounds as antitumoral drugs. Here, we describe the signaling pathway that mediates cannabinoid-induced apoptosis of tumor cells. By using a wide array of experimental approaches, we identify the stress-regulated protein p8 (also designated as candidate of metastasis 1) as an essential mediator of cannabinoid antitumoral action and show that p8 upregulation is dependent on de novo-synthesized ceramide. We also observe that p8 mediates its apoptotic effect via upregulation of the endoplasmic reticulum stress-related genes ATF-4, CHOP, and TRB3. Activation of this pathway may constitute a potential therapeutic strategy for inhibiting tumor growth.

Introduction

The hemp plant *Cannabis sativa* produces approximately 60 unique compounds known as cannabinoids, of which Δ^9-tetrahydrocannabinol (THC) is the most important, owing to its high potency and abundance in cannabis (Gaoni and Mechoulam, 1964). THC exerts a wide variety of biological effects by mimicking endogenous substances—the endocannabinoids anandamide (Devane et al., 1992) and 2-arachidonoylglycerol (Mechoulam et al., 1995)—that bind to and activate specific cannabinoid receptors. So far, two cannabinoid-specific $G_{i/o}$ protein-coupled receptors have been cloned and characterized from mammalian tissues (Howlett et al., 2002): CB_1 (Matsuda et al., 1990), particularly abundant in the brain, and CB_2 (Munro et al., 1993), mainly expressed in the immune system.

One of the most exciting areas of current research in the cannabinoid field is the study of the potential application of cannabinoids as therapeutic agents (Di Marzo et al., 2004; Piomelli, 2003). Among these possible applications, cannabinoids are being investigated as potential antitumoral drugs (Guzman, 2003).

Thus, cannabinoid administration has been shown to curb the growth of several models of tumor xenografts in rats and mice (Guzman, 2003). This antitumoral action of cannabinoids relies, at least in part, on their ability to induce apoptosis of tumor cells (Casanova et al., 2003; Galve-Roperh et al., 2000; McKallip et al., 2002; Ruiz et al., 1999; Sanchez et al., 1998; Sarfaraz et al., 2005). In addition, cannabinoids have been shown to inhibit tumor angiogenesis (Blazquez et al., 2003, 2004; Portella et al., 2003). Studies conducted in glioma (Blazquez et al., 2004; Galve-Roperh et al., 2000; Gomez del Pulgar et al., 2002a) and prostate tumor (Mimeault et al., 2003) cells support that the antitumoral effect of cannabinoids is associated with an accumulation of the proapoptotic sphingolipid ceramide (Ogretmen and Hannun, 2004). However, the downstream targets of this metabolite and the participation of additional signaling pathways in the proapoptotic effect of cannabinoids remain to be elucidated. Here, we used tumor cells with different sensitivity to cannabinoid-induced apoptosis to investigate the molecular mechanisms involved in the antitumoral action of these compounds.

SIGNIFICANCE

Marijuana has been used in medicine for many centuries, and nowadays there is a renaissance in the study of the therapeutic effects of cannabinoids. One of the most active areas of research in the cannabinoid field is the study of the potential antitumoral application of these drugs. Our results unravel the mechanism of cannabinoid antitumoral action by demonstrating the proapoptotic role of the stress protein p8 via its downstream targets ATF-4, CHOP, and TRB3. The identification of this pathway may contribute to the design of therapeutic strategies for inhibiting tumor growth. In particular, our findings can help to improve the efficiency and selectivity of potential antitumoral therapies with cannabinoids.

Results

THC-induced apoptosis involves upregulation of several stress-regulated genes

We used two subclones of C6 glioma cells designated as C6.9 and C6.4 as a first step to investigate the proapoptotic action of THC. C6.4 cells exhibit a lower sensitivity to cannabinoid-induced apoptosis than C6.9 cells (Figure 1A and Galve-Roperh et al., 2000). By using DNA arrays, we analyzed the gene expression profile of C6.9 and C6.4 cells in response to THC (1.6 μM) at a time point (18 hr) at which no changes in viability were evident yet (Figure 1B, inset). The entire list of genes that were differentially expressed in THC-treated C6.9 and C6.4 cells as compared with their corresponding controls can be found as Tables S1 and S2 in the Supplemental Data available with this article online. Data analysis showed a series of stress-associated genes that were selectively upregulated in C6.9 but not C6.4 cells (Figure 1B). One of these genes was that encoding the stress-regulated protein p8 (also known as candidate of metastasis 1), a protein that belongs to the family of HMG-I/Y transcription factors and that has been previously implicated in the control of cell fate (Jiang et al., 2005b; Malicet et al., 2003; Su et al., 2001; Vasseur et al., 2002a). By using real-time quantitative PCR, we confirmed that THC upregulates p8 mRNA levels in C6.9 but not in C6.4 cells (Figure 1C). Likewise, Western blot analysis showed that THC increases p8 protein levels in C6.9 but not in C6.4 cells (Figure 1D). As accumulation of de novo-synthesized ceramide has been implicated in the mechanism of cannabinoid-induced apoptosis of glioma cells (Galve-Roperh et al., 2000; Gomez del Pulgar et al., 2002a), we tested whether ceramide accumulation is involved in the regulation of p8. Preincubation with 1 μM ISP-1—a selective inhibitor of serine palmitoyltransferase, the enzyme that catalyzes the rate-limiting step of sphingolipid biosynthesis—prevented THC-induced p8 upregulation (Figure 1E).

p8 mediates THC-induced apoptosis

We next investigated the involvement of p8 in THC-induced apoptosis of human tumor cells. THC treatment decreased viability, activated caspase 3, and induced p8 in astrocytoma U87MG, oligodendroglioma Gos3, pancreatic cancer MiaPaCa2, and melanoma A375 cells (Figure S1), supporting the idea that p8 upregulation may be a general event in THC-induced apoptosis. We selected U87MG cells for further studies and verified that THC induces apoptosis of these cells (Figure S2A) and that mitochondria (Figures S2B and S2C) and caspases (Figure S2D) are involved in this effect.

Incubation of U87MG cells with ISP-1 (1 μM), the selective CB$_1$ receptor antagonist SR141716 (1 μM), or the selective CB$_2$ receptor antagonist SR144528 (1 μM) prevented cell death (Figure 2A) and ceramide accumulation (Figure 2B). We confirmed that ceramide is involved in the regulation of p8 also in these cells, as pharmacological inhibition of ceramide synthesis de novo reduced by ~50% the THC-triggered increase in p8 levels (Figure 2C). Likewise, incubation of U87MG cells with the ceramide analog C$_2$-ceramide (3 μM; 18 hr) increased p8 mRNA expression (Figure 2D). Since conversion to complex sphingolipids has been implicated in the regulation of the proapoptotic role of ceramide (Gouaze et al., 2005; Ogretmen and Hannun, 2004), we investigated whether cannabinoid treatment affected accumulation of these sphingolipids. Selective
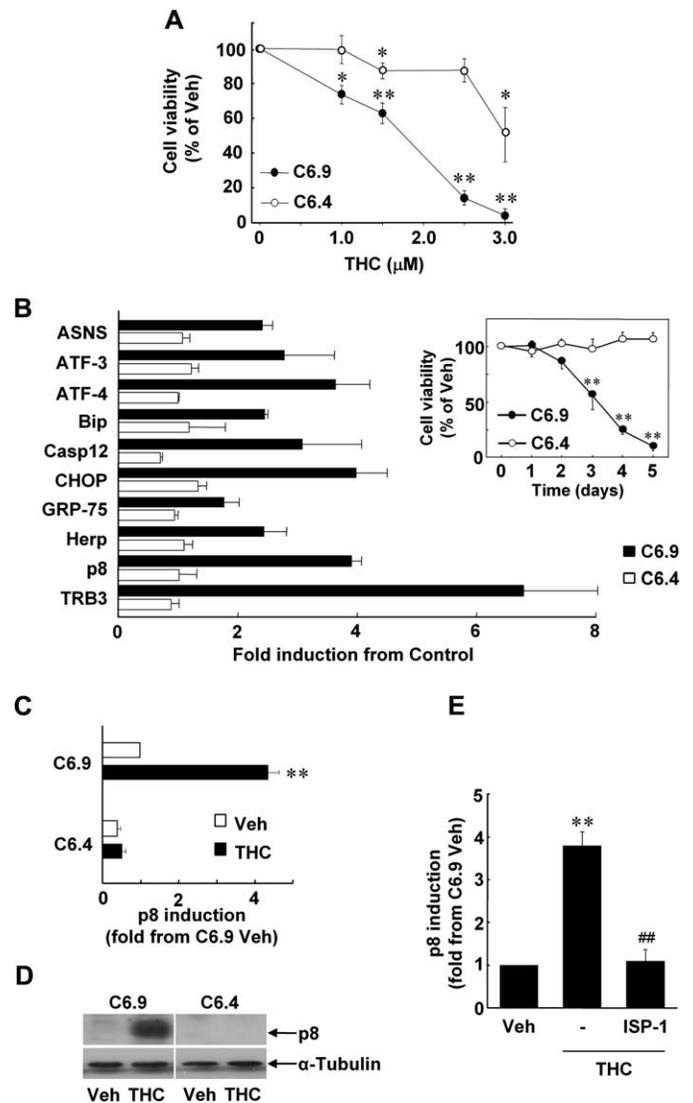
Figure 1. p8 is upregulated in cannabinoid-sensitive glioma cells

A: Effect of THC on C6.9 and C6.4 cell viability after 72 hr of treatment (n = 6; **p < 0.01 and *p < 0.05 from vehicle-treated cells).

B: Stress-related genes differentially upregulated in the gene array analysis of THC-treated C6.9 versus C6.4 cells (n = 3). ASNS, asparagine synthetase. Inset: effect of THC (1.6 μM) on C6.9 and C6.4 cell viability (n = 6; **p < 0.01 from vehicle-treated cells).

C: Effect of THC on p8 mRNA levels (as determined by real-time quantitative PCR) in C6.9 and C6.4 cells (n = 3; **p < 0.01 from vehicle-treated C6.9 cells).

D: Effect of THC on p8 protein expression in C6.9 and C6.4 cells (n = 2; a representative Western blot experiment is shown).

E: Effect of ISP-1 on THC-induced p8 expression of C6.9 cells (n = 4; **p < 0.01 from vehicle-treated cells; ##p < 0.01 from THC-treated cells).

Data in **A–C** and **E** are expressed as mean ± standard deviation. (Bars correspond to standard deviation.)

knockdown (Figure 2E) or pharmacological inhibition (Figure 2F) of glucosylceramide synthase (GCS)—the enzyme that catalyzes the rate-limiting step of glycosphingolipid biosynthesis (Ogretmen and Hannun, 2004)—did not significantly modify the effect of THC on cell viability or p8 expression (data not shown). In addition, THC did not produce major changes in U87MG glycosphingolipid profile (Figure 2G), suggesting
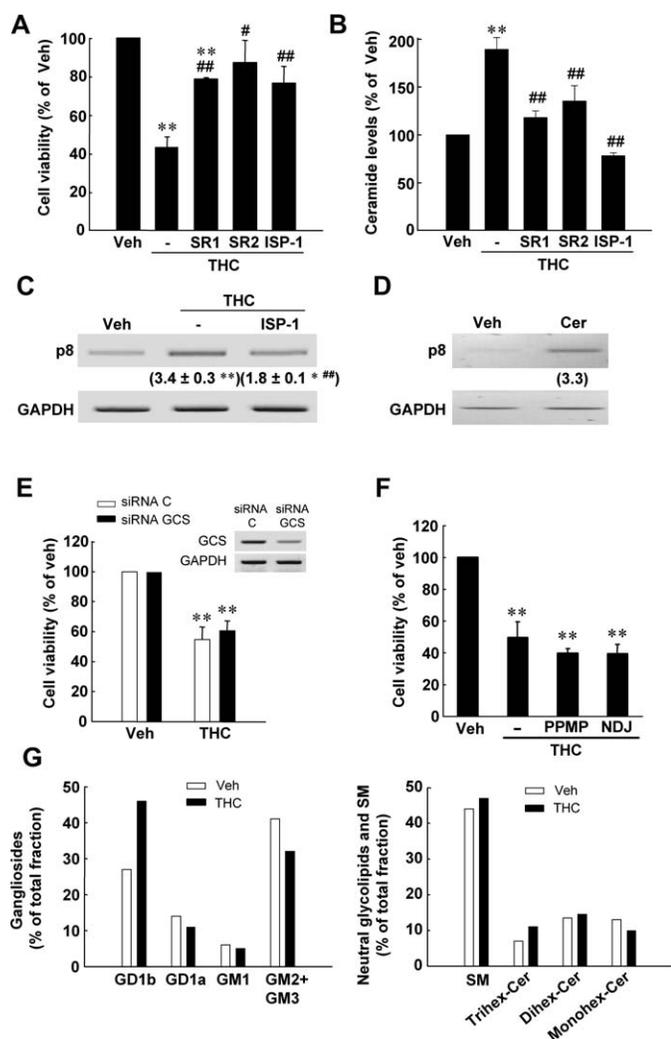
Figure 2. De novo-synthesized ceramide mediates THC-induced p8 upregulation and apoptosis

A: Effect of THC on the viability of U87MG cells preincubated with vehicle, SR141716 (SR1), SR144528 (SR2), or ISP-1 (n = 4; **p < 0.01 from vehicle-treated cells; ##p < 0.01 and #p < 0.05 from THC-treated cells).

B: Effect of THC on ceramide levels of U87MG cells preincubated with vehicle, SR1, SR2, or ISP-1 (n = 3; **p < 0.01 from vehicle-treated cells; ##p < 0.01 from THC-treated cells).

C: Effect of ISP-1 on THC-induced upregulation of p8 mRNA levels (n = 6; a representative RT-PCR experiment is shown). Values of gene induction as determined by real-time quantitative PCR (expressed as mean fold increase ± SD relative to vehicle-treated cells; n = 6; **p < 0.01 and *p < 0.05 from vehicle-treated cells; ##p < 0.01 from THC-treated cells) are shown in parentheses.

D: Effect of C_2-ceramide on p8 mRNA levels (n = 3; a representative RT-PCR experiment is shown). Values of gene induction as determined by real-time quantitative PCR (expressed as fold increase relative to vehicle-treated cells in that experiment) are shown in parentheses.

E: Effect of THC on the viability of U87MG cells transfected with a control (siRNAC) or a GCS-selective (siRNA GCS) siRNA (n = 3; **p < 0.01 from vehicle-treated cells). Upper panel: a representative RT-PCR of siRNAC and siRNA GCS vehicle-treated cells is shown.

F: Effect of THC on the viability of U87MG cells preincubated with vehicle, 1 μM DL-Threo-1-phenyl-2-palmitoylamino-3-morpholino-1-propanol (PPMP) or 200 μM N-(n-butyl)deoxynojirimycin (NDJ) (n = 6; **p < 0.01 from vehicle-treated cells).

G: Effect of THC on the glycosphingolipid profile of U87MG cells. A representative experiment of two is shown. Total dpm in the ganglioside fraction: Veh = 32134, THC = 29129. Total dpm in the neutral glycolipid fraction:

that conversion of ceramide to complex sphingolipids does not play a major role in the proapoptotic effect of THC.

To determine the role of p8 in the triggering of THC-induced apoptosis, we employed siRNA to selectively reduce the expression of this protein. Knockdown of p8 mRNA levels prevented U87MG cell death induced by both THC (Figure 3A) and C_2-ceramide (3 μM; 24 hr; Figure 3B). In addition, pharmacological blockade of the mitochondrial respiratory chain prevented THC-induced cell death (Figure S2B) but not p8 upregulation (Figure 3D), supporting an early premitochondrial role for p8 in THC-induced apoptosis. To further support the involvement of p8 in the proapoptotic effect of THC, we used $p8^{+/+}$ and $p8$-deficient Ras^{V12}/E1A-transformed mouse embryonic fibroblasts (MEFs) (Vasseur et al., 2002b) (we verified that these express CB receptors; Figure S3A). THC (7 μM) induced apoptosis (72 hr, Figure 3C; 48 hr, Figure S3B) and decreased the mitochondrial membrane potential (18 hr, Figure 3E) of $p8^{+/+}$ but not $p8$-deficient cells.

p8 controls several endoplasmic reticulum stress-regulated genes to induce apoptosis

To investigate the downstream targets of p8 that participate in its proapoptotic action, we first analyzed the gene expression profile of $p8$-deficient MEFs infected with an empty or a p8-overexpressing retroviral vector. The entire list of genes that were differentially expressed in the p8-overexpressing cells can be found as Table S3. Interestingly, when we compared the genes selectively modulated in p8-overexpressing MEFs with those selectively modulated by THC in cannabinoid-sensitive glioma cells, we found several common ones, including those encoding the activating transcription factor-4 (ATF-4) and the stress-regulated protein tribbles homolog 3 (TRB3, also known as cell death-inducible kinase, NIPK, and SKIP3) (Figure 4A), that are involved in the response to endoplasmic reticulum (ER) stress (Ohoka et al., 2005). We confirmed by real-time quantitative PCR that THC upregulates ATF-4 and TRB3 in C6.9 but not in C6.4 cells (Figure 4B). In addition, C6.4 cells forced to overexpress p8 in a stable fashion exhibited increased levels of ATF-4 and TRB3 mRNA (Figure 4C). Moreover, ATF-4 and TRB3 mRNA levels were lower in $p8$-deficient MEFs than in their corresponding $p8^{+/+}$ counterparts (Figure 4D).

It has been recently shown that ATF-4 cooperates with C/EBP homologous protein (CHOP, also known as DDIT3) (Ma et al., 2002) to regulate TRB3 as part of the ER stress apoptotic pathway (Ohoka et al., 2005). In U87MG cells, THC induced upregulation of ATF-4, CHOP, and TRB3 mRNA levels (Figure 5A), an effect that was reduced by knockdown of p8 expression (Figure 5A) or incubation with ISP-1 (Figure 5B). Likewise, incubation of U87MG cells with the ceramide analog C_2-ceramide (3.0 μM; 18 hr) increased ATF-4, CHOP, and TRB3 mRNA expression (Figure 5C). Moreover, THC treatment induced ATF-4, CHOP, and TRB3 upregulation in $p8^{+/+}$ but not in $p8$-deficient transformed MEFs (Figure 5D), further confirming the involvement of p8 in the cannabinoid-induced upregulation of these genes.

Veh = 129765, THC = 73357. SM, sphingomyelin; Trihex-Cer, trihexosylceramide; Dihex-Cer, dihexosylceramide; Monohex-Cer, monohexosylceramide.
Data in A–C, E, and F are expressed as mean ± standard deviation. (Bars in A, B, E, and F correspond to standard deviation.)

To test whether these ER stress-related proteins were involved in cannabinoid-induced apoptosis, we selectively knocked down ATF-4 and TRB3 mRNA levels in U87MG cells. siRNA for either ATF-4 (Figure 5E) or TRB3 (Figure 5F) blunted THC-induced cell death, indicating that THC triggers a p8-mediated response that involves ATF-4, CHOP, and TRB3 upregulation to induce apoptosis (Figure 5G).

Activation of the ER stress pathway sensitizes tumor cells to apoptosis

Next, we studied whether enforced expression of p8 or TRB3 affected the viability of the cannabinoid-resistant cell line C6.4. p8 or TRB3 overexpression did not induce apoptosis by itself (data not shown) but sensitized these cells to a further cannabinoid treatment (Figures 6A and 6B). p8-overexpressing C6.4 cells also became sensitized to the ER stress inducers tunicamycin and thapsigargin (data not shown). In addition, *p8*-deficient transformed MEFs were more resistant to tunicamycin and thapsigargin than their corresponding *p8*^{+/+} counterparts (Figures 6C and 6D), supporting an important role for p8 in the response to ER stress. We therefore studied the cooperative action of THC with these agents as well as with cisplatin and doxorubicin—two frequently used chemotherapeutic drugs. Submaximal doses of thapsigargin, cisplatin, or doxorubicin and THC reduced U87MG cell viability in a synergic fashion (Figures 6E, 6G, and 6H). An additive effect was observed when tunicamycin and THC were administered to these cells (Figure 6F).

We subsequently tested whether the aforementioned cannabinoid effects were selective of tumor cells. Of interest, THC challenge of astrocytes, the normal counterparts of astrocytoma cells, did not affect either viability or expression of *p8*, *ATF-4*, *TRB3*, and other ER stress-related genes (Figure S4), indicating that cannabinoid treatment does not activate the proapoptotic route described above in nontransformed cells.

THC treatment leads to p8 upregulation in vivo

To give further relevance to these findings, we generated tumors by subcutaneously injecting human U87MG astrocytoma cells in mice. Administration of THC (15 mg/kg/day, 14 days) significantly reduced tumor growth (Figure 7A) and increased apoptosis (Figure 7B) in these tumors. This correlated with increased immunostaining (Figure 7C) and mRNA levels (Figure 7D) of p8. Activation of this pathway was further confirmed by the upregulation of TRB3 (Figure 7D).

In order to confirm the in vivo relevance of p8 in the cannabinoid-induced ER stress-dependent proapoptotic action, we generated tumors by subcutaneously injecting *p8*^{+/+} or *p8*-deficient transformed MEFs. THC (15 mg/kg/day, 8 days) significantly reduced tumor growth and induced apoptosis of *p8*^{+/+}

Figure 3. p8 is required for THC-induced apoptosis

A: Effect of THC on the viability of U87MG cells transfected with a control (siRNAC) or a p8-selective (siRNAp8) siRNA (n = 6). Upper panel: real-time quantitative PCR analysis of p8 mRNA levels in siRNAC-and siRNAp8-transfected cells (n = 3; a representative RT-PCR of siRNAC and siRNAp8 vehicle-treated cells is shown). **p < 0.01 and *p < 0.05 from vehicle-treated cells; ##p < 0.01 from the corresponding siRNAC-transfected cells.

B: Effect of C$_2$-ceramide on the viability of U87MG cells transfected with siRNAC or siRNAp8 (n = 3; **p < 0.01 from vehicle-treated cells; #p < 0.05 from C$_2$-ceramide-treated siRNAC cells).

C: Effect of THC on the viability of *p8*^{+/+} and *p8*-deficient Ras^{V12}/E1A-transformed MEFs (n = 5; **p < 0.01 and *p < 0.05 from vehicle-treated cells; ##p < 0.01 from THC-treated MEF *p8*^{+/+} cells). Upper panel: effect of THC on p8 expression of *p8*^{+/+}and *p8*-deficient cells (n = 2; a representative RT-PCR experiment is shown).

D: Effect of rotenone on THC-induced upregulation of p8 mRNA levels (n = 3; a representative RT-PCR experiment is shown). Values of gene induction as determined by real-time quantitative PCR (expressed as fold increase relative to vehicle-treated cells in that experiment) are shown in parentheses.

E: Effect of THC on mitochondrial membrane potential of *p8*^{+/+} (upper panels) or *p8*-deficient (lower panels) Ras^{V12}/E1A-transformed MEFs (n = 3; *p < 0.05 from vehicle-treated cells. A dot plot of a representative experiment is shown in the right panels. Values in the lower left corner of each plot correspond to the percentage of low TMRM/Hoechst-negative cells in that experiment.

Data in **A**–**C** and **E** are expressed as mean ± standard deviation. (Bars correspond to standard deviation.)
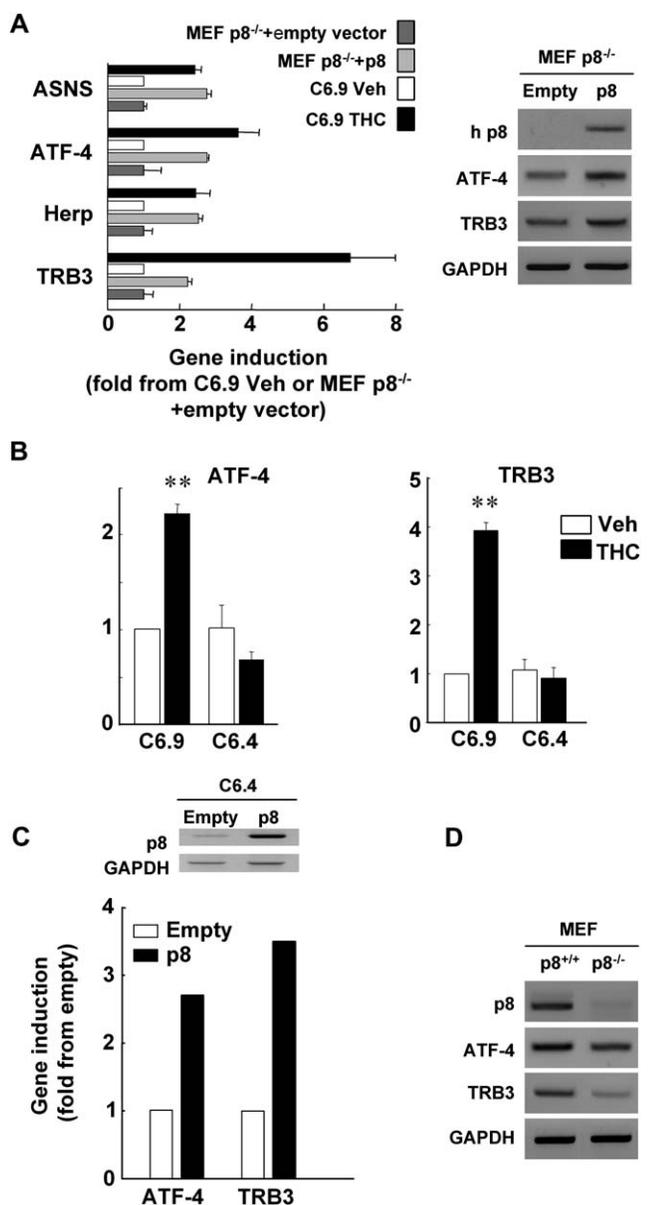
Figure 4. p8 controls ATF-4 and TRB3 to induce apoptosis

A: Genes differentially expressed in p8-overexpressing $Ras^{V12}/E1A$-transformed $p8^{-/-}$ MEF and THC-treated C6.9 cells. Results are expressed as mean fold induction ± SD relative to empty vector-infected MEFs or to vehicle-treated C6.9 cells. ASNS, asparagine synthetase. Right panel: ATF-4 and TRB3 mRNA levels of p8-deficient $Ras^{V12}/E1A$-transformed MEFs infected with an empty or a (human) p8-overexpressing vector (n = 3; a representative RT-PCR is shown). h p8, probe for human p8.

B: Effect of THC on ATF-4 and TRB3 mRNA levels (as determined by real-time quantitative PCR) in C6.9 and C6.4 cells (n = 3; **$p < 0.01$ from vehicle-treated C6.9 cells).

C: Effect of p8 overexpression on ATF-4 and TRB3 mRNA levels (as determined by real-time quantitative PCR) of C6.4 cells. A representative experiment is shown. Upper panel: analysis of h p8 mRNA levels in cells infected with empty and p8-overexpressing retroviral vector (a representative RT-PCR experiment is shown).

D: ATF-4 and TRB3 mRNA levels of $p8^{+/+}$ and p8-deficient $Ras^{V12}/E1A$-transformed MEFs (n = 3; a representative RT-PCR is shown).

Data in **A** and **B** are expressed as mean ± standard deviation. (Bars correspond to standard deviation.)

(Figures 7E and 7F) but not of *p8*-deficient (Figures 7G and 7H) tumors.

We next studied the involvement of the p8 pathway in the antitumoral action of THC in astrocytoma cells obtained from patient biopsies. Cells obtained from human glioblastoma 1 (HG1) were more sensitive to the cannabinoid than cells obtained from human glioblastoma 2 (HG2) (Figure 8A). Likewise, upregulation of p8, ATF-4, CHOP, and TRB3 in response to THC (6 μM; 18 hr) was higher in HG1 than in HG2 cells (Figure 8B). Finally, we analyzed the tumors of two patients enrolled in a clinical trial aimed at investigating the effect of THC on recurrent glioblastoma multiforme. The patients were subjected to local THC administration, and biopsies were taken before and after the treatment. In the two patients, both apoptosis (Figure 8C) and p8 immunoreactivity (Figure 8D) were increased after cannabinoid inoculation.

Discussion

Cannabinoids have been shown to exert antiproliferative actions on a wide spectrum of tumor cells. Data presented here now shed light on the mechanism responsible for these actions by elucidating the signaling pathway that mediates cannabinoid-induced apoptosis. In particular, different observations strongly support a major role for the stress-regulated protein p8 in the triggering of THC proapoptotic action: (1) THC leads to p8 upregulation and apoptosis in several tumor cells as well as in cells obtained from human astrocytoma biopsies; (2) p8 upregulation does not occur in cannabinoid-resistant tumor cells; (3) *p8*-deficient cells or cells which p8 mRNA levels have been selectively knocked down are resistant to cannabinoid-induced apoptosis; (4) p8 overexpression renders cannabinoid-resistant tumor cells sensitive to THC; (5) THC administration upregulates p8 in tumors in vivo; and (6) *p8*-deficient tumors are resistant to the proapoptotic action of cannabinoids.

p8 belongs to the family of HMG-I/Y transcription factors and was originally described as a gene induced during the acute phase of pancreatitis (Mallo et al., 1997). Intriguingly, p8 seems to play a dual role in the control of cell fate. On the one hand—and in line with the results presented here—p8 has been implicated in a reduction of cell proliferation of pancreatic (Malicet et al., 2003 and our unpublished observations) and breast (Jiang et al., 2005a) tumor cells. On the other hand, expression of this protein is necessary for the establishment of newly generated tumors (Vasseur et al., 2002a). In addition, p8 overexpression has been associated inversely to apoptosis in samples obtained from biopsies of pancreatic (Su et al., 2001) and breast cancer (Ito et al., 2005) but also directly to improved prognosis of breast cancer (Jiang et al., 2005b). All these observations suggest that cell or tissue-specific factors may determine the final role played by p8 in the control of cell fate. In line with this idea, by using the yeast two-hybrid system we have recently identified several p8-interacting proteins including c-Jun activation domain binding protein 1 (JAB1) and prothymosin α (J.L.I. and C.M., unpublished data), both of which have been implicated in the control of cell proliferation and apoptosis (Emberley et al., 2005; Jiang et al., 2003). Thus, modulation of the levels or the activity of these or other proteins in a particular cellular or tumoral context could be one of the factors involved in determining the final biological role of p8. In agreement with this
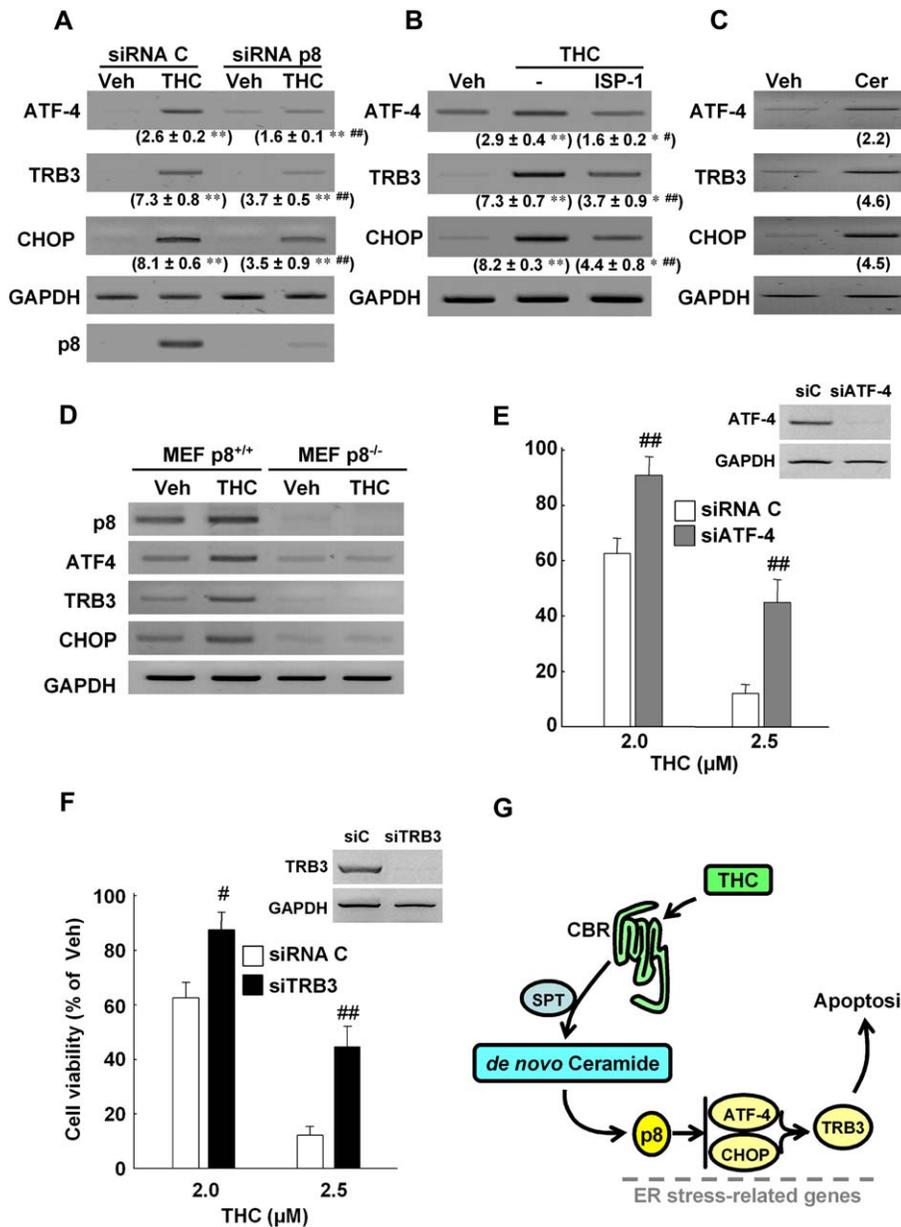
Figure 5. THC induces apoptosis via p8-dependent ATF-4, CHOP, and TRB3 upregulation

A: Effect of p8 knockdown on THC-induced ATF-4, CHOP, and TRB3 upregulation in U87MG cells (n = 6; a representative RT-PCR experiment is shown). Values of gene induction as determined by real-time quantitative PCR (expressed as mean fold increase ± SD relative to vehicle-treated cells; n = 6; **p < 0.01 from vehicle-treated cells; ##p < 0.01 from siRNAC THC-treated cells) are shown in parentheses.

B: Effect of ISP-1 on ATF-4, CHOP, and TRB3 mRNA levels of U87MG cells (n = 6; a representative RT-PCR experiment is shown). Values of gene induction as determined by real-time quantitative PCR (expressed as fold increase ± SD relative to vehicle-treated cells; **p < 0.01 and *p < 0.05 from vehicle-treated cells; ##p < 0.01 and #p < 0.05 from THC-treated cells) are shown in parentheses.

C: Effect of C_2-ceramide on ATF-4, CHOP, and TRB3 mRNA levels of U87MG cells (n = 3; a representative RT-PCR experiment is shown). Values of gene induction as determined by real-time quantitative PCR (expressed as fold increase relative to vehicle-treated cells in that experiment) are shown in parentheses.

D: Effect of THC on p8, ATF-4, CHOP, and TRB3 mRNA levels of p8^{+/+} and p8-deficient Ras[V12]/E1A-transformed MEFs (n = 3; a representative RT-PCR is shown).

E and F: Effect of THC on the viability of U87MG cells transfected with siRNAC, ATF-4-selective (siATF-4), or TRB3-selective (siTRB3) siRNA (n = 6; ##p < 0.01 and #p < 0.05 from siRNAC THC-treated cells). Upper panels: Analysis of ATF-4 (**E**) or TRB3 (**F**) mRNA levels in cells transfected with siRNAC and siATF-4 (**E**) or with siRNAC and siTRB3 (**F**). Representative RT-PCR experiments are shown.

G: The panel shows a schematic of the proposed mechanism of THC-induced apoptosis of tumor cells. THC binds to CB receptors and stimulates ceramide synthesis de novo via activation of serine pamitoyltransferase (SPT). Ceramide accumulation leads to upregulation of p8 and in turn of the ER stress-related genes ATF-4, CHOP, and TRB3. Activation of this pathway induces apoptosis of tumor cells.

Data in **E** and **F** are expressed as mean ± standard deviation. (Bars in **E** and **F** correspond to standard deviation.)

idea, stable overexpression of p8 sensitizes cannabinoid-resistant tumor cells to a further proapoptotic stimulus but is not enough to induce apoptosis by itself, suggesting that an alternative pathway that would be triggered by THC in cannabinoid-resistant tumor cells may also be required—together with p8 upregulation—to produce a proapoptotic signal.

Although the molecular mechanisms whereby p8 mediates its effects are not well established yet, it has been postulated that this protein may act as a cotranscription factor to regulate gene expression (Hoffmeister et al., 2002; Jiang et al., 2005a; Garcia-Montero et al., 2001). In this report, analysis of gene expression profiles together with knockdown experiments has led us to identify three genes—those encoding the transcription factors ATF-4 and CHOP and the stress-related pseudokinase TRB3—as p8-modulated genes in apoptosis. Of interest, ATF-4 and CHOP have been shown to regulate the expression of TRB3 in response to ER stress to induce apoptosis of human

tumor cells (Ohoka et al., 2005). A series of ER alterations such as calcium depletion, protein misfolding, and impairment of protein trafficking to the Golgi triggers the ER stress response (Schroder and Kaufman, 2005). When these ER alterations cannot be repaired by this response, the damaged cells undergo apoptosis. Several stimuli, including ischemia (Tajiri et al., 2004), viral infection (Benali-Furet et al., 2005; Li et al., 2005), and drugs such as tunicamycin (Ohoka et al., 2005) or cisplatin (Mandic et al., 2003) induce apoptosis through this pathway, which may play an important role in the control of tumor growth (Ma and Hendershot, 2004). Detailed gene expression analysis of THC-challenged glioma cells demonstrates that several proteins related with the ER response (including caspase 12, Bip [also designated as GRP-78], asparagine synthetase, and Herp—in addition to the aforementioned CHOP, ATF-4, and TRB3) are selectively upregulated in cannabinoid-sensitive cells. In line with this observation, genetic downregulation of
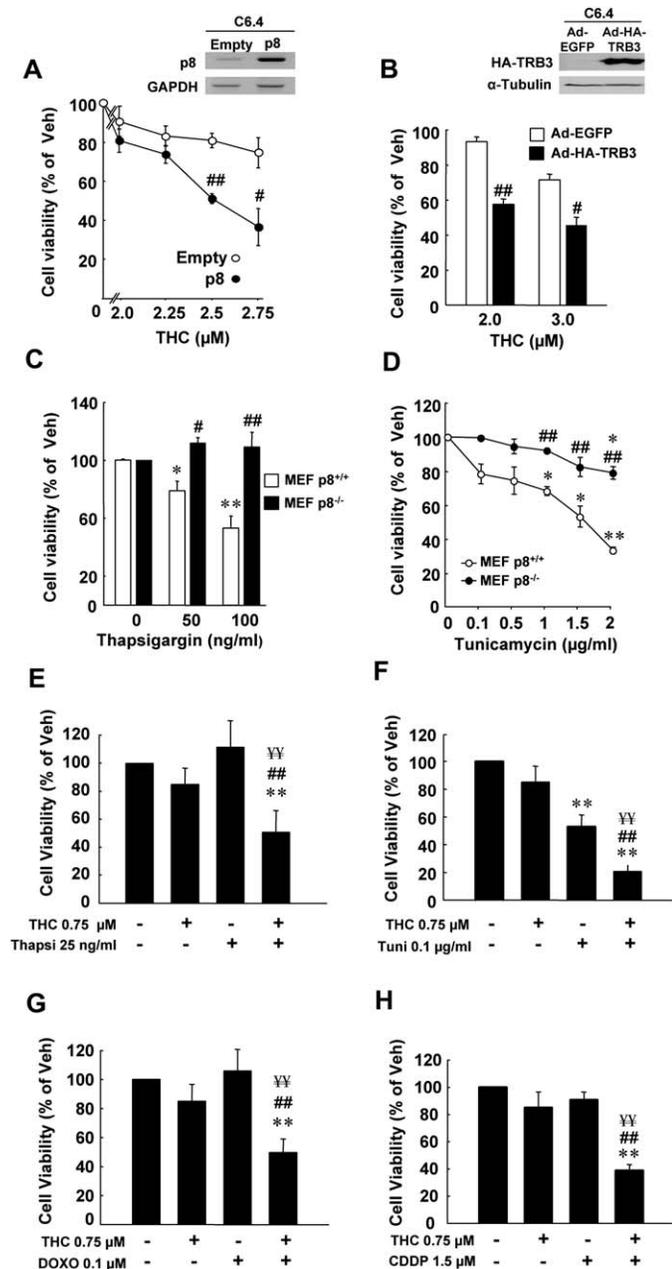
Figure 6. THC and ER stress inducers act in a synergistic fashion on tumor cells

A: Effect of THC on the viability of C6.4 cells infected with an empty or a p8-overexpressing retroviral vector (n = 6; $^{##}p < 0.01$ and $^{#}p < 0.05$ from cells infected with the empty vector). Upper panel: analysis of p8 mRNA levels in cells infected with empty and p8-overexpressing retroviral vector (a representative RT-PCR experiment is shown).

B: Effect of THC on the viability of C6.4 cells infected with an EGFP (Ad-EGFP) or a hemagglutinin-tagged-TRB3 (Ad-HA-TRB3)-overexpressing adenoviral vector (n = 5; $^{##}p < 0.01$ and $^{#}p < 0.05$ from Ad-EGFP-infected cells). Upper panel: analysis of HA-TRB3 expression in Ad-EGFP and Ad-HA-TRB3-infected cells (a representative Western blot experiment is shown).

C: Effect of thapsigargin on cell viability of $p8^{+/+}$ and p8-deficient Ras^{V12}/E1A-transformed MEFs (n = 4; $^{**}p < 0.01$ and $^{*}p < 0.05$ from vehicle-treated cells; $^{##}p < 0.01$ and $^{#}p < 0.05$ from the corresponding thapsigargin-treated $p8^{+/+}$ cells).

D: Effect of tunicamycin on cell viability of $p8^{+/+}$ and p8-deficient Ras^{V12}/E1A-transformed MEFs (n = 4; $^{**}p < 0.01$ and $^{*}p < 0.05$ from vehicle-treated cells; $^{##}p < 0.1$ from the corresponding tunicamycin-treated $p8^{+/+}$ cells).

ATF-4 and TRB3 mRNA levels reduces THC-induced cell death, and TRB3 overexpression sensitizes cannabinoid-resistant cells to THC-induced apoptosis. Taken together, these findings strongly support a major role for the ER stress response in the proapoptotic action of cannabinoids on tumor cells.

Accumulation of de novo-synthesized ceramide has been implicated in the proapoptotic action of cannabinoids in glioma cells (Blazquez et al., 2004; Galve-Roperh et al., 2000; Gomez del Pulgar et al., 2002a). Moreover, ceramide levels have been inversely associated with malignant progression of human glial tumors (Riboni et al., 2002). However, the molecular mechanism whereby ceramide mediates these actions has remained elusive. Our findings show that de novo-synthesized ceramide is involved in the upregulation of p8 and its downstream targets, and that p8 may be a component of the ceramide proapoptotic cascade. Although accumulation of complex sphingolipids had been implicated in activation of the ER stress pathway (Tessitore et al., 2004), we did not observe major changes in the glycosphingolipid profile of our cells upon cannabinoid treatment. Moreover, inhibition of GCS—the enzyme that catalyzes the rate-limiting step of glycosphingolipid biosynthesis—did not change the response to cannabinoid treatment of tumor cells. Taken together, these observations support a role for ceramide rather than for glycosphingolipids in the proapoptotic effect of THC.

In this report, we show that the proapoptotic effect of cannabinoids on tumor cells is mediated by a ceramide-dependent upregulation of the stress protein p8 and several downstream targets (ATF-4, CHOP, and TRB3) related with the ER stress proapoptotic pathway (Figure 5G). Moreover, we provide evidence that p8 upregulation also takes place in vivo and that resistance to cannabinoid treatment is associated with a decreased activation of the p8-regulated proapoptotic pathway. Our results also support that cannabinoid treatment does not activate this pathway in nontransformed cells, in line with the belief that cannabinoid proapoptotic action is selective for tumor versus nontumor cells (Guzman, 2003), and that cannabinoids act in a synergic fashion with ER stress inducers as well as with other antitumoral agents. Efficacious treatment of cancer will require in the future the use of selective strategies, including most likely the combination of several drugs and therapeutic approaches. The identification of the p8-regulated pathway described here may contribute to the design of therapeutic strategies for inhibiting tumor growth. In particular, our findings can help to improve the efficiency and selectivity of a potential cannabinoid-based antitumoral therapy.

Experimental procedures

Reagents

Z-DQMD-FMK (caspase 3 inhibitor), Z-VAD-FMK (pan-caspase inhibitor), rotenone, N-(n-butyl)deoxynojirimycin (NDJ), and DL-Threo-1-phenyl-2-palmitoylamino-3-morpholino-1-propanol (PPMP) were from Sigma Chemical

E–H: Effect of THC and thapsigargin (**E**), tunicamycin (**F**), doxorubicin (**G**), or cisplatin (**H**; CDDP) on viability of U87MG cells (**E**, n = 4; **F**, n = 4; **G**, n = 4; **H**, n = 4; $^{**}p < 0.01$ from vehicle-treated cells; $^{##}p < 0.01$ from THC-treated cells; $^{¥¥}p < 0.01$ from the corresponding thapsigargin [**E**]-, tunicamycin [**F**]-, doxorubicin [**G**]-, or cisplatin [**H**]-treated cells).

Data in **A–H** are expressed as mean ± standard deviation. (Bars correspond to standard deviation.)
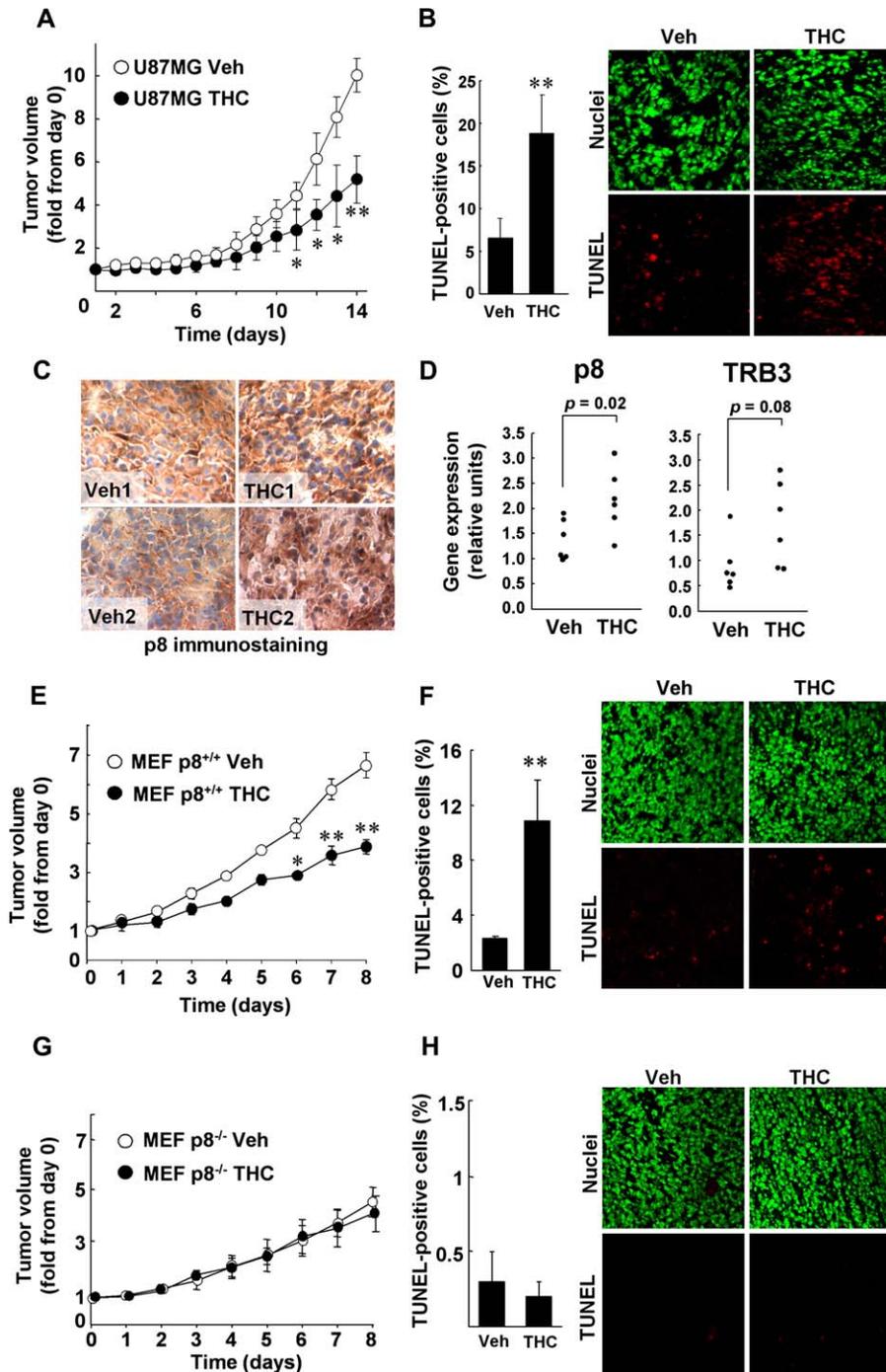
Figure 7. p8 mediates THC antitumoral action in tumor xenografts

A: Effect of THC administration on the growth of U87MG-cell tumor xenografts in nude mice (n = 8 for each condition; **p < 0.01 and *p < 0.05 from vehicle-treated tumors). **B:** Effect of THC administration on apoptosis of U87MG-cell tumor xenografts. Results correspond to three dissected tumors for each condition and are expressed as the percentage of TUNEL-positive cells relative to the total number of cells in each section (**p < 0.01 from vehicle-treated tumors; a representative photomicrograph is shown). **C:** Immunohistochemical analysis of p8 expression in U87MG-cell tumor xenografts. Representative photomicrographs of p8 immunostaining (dark brown) in sections of two tumors treated with vehicle (left panels) or THC (right panels) are shown. **D:** p8 and TRB3 mRNA expression (as determined by real-time quantitative PCR) in U87MG-cell tumor xenografts. The plot represents gene expression (in fold number) of each individual tumor relative to one of the vehicle-treated tumors. (n = 6 for each condition). **E and G:** Effect of THC administration on the growth of $p8^{+/+}$ (**E**) or $p8$-deficient (**G**) Ras^{V12}/E1A-transformed MEF-tumor xenografts in nude mice (**E**, n = 3 for each condition; **F**, n = 6 for each condition; **p < 0.01 and *p < 0.05 from vehicle-treated tumors). **F and H:** Effect of THC administration on apoptosis of $p8^{+/+}$ (**F**) and $p8$-deficient (**H**) Ras^{V12}/E1A-transformed MEF-tumor xenografts. Results correspond to three dissected tumors for each condition and are expressed as the percentage of TUNEL-positive cells relative to the total number of cells in each section (**p < 0.01 from vehicle-treated tumors; representative photomicrographs are shown). Data in **A**, **B**, and **E–H** are expressed as mean ± standard deviation. (Bars correspond to standard deviation.)

Co (St. Louis, MO). Myriocin (ISP-1) was from Biomol (Plymouth Meeting, PA). Radiochemicals were from Amersham Biosciences (Piscataway, NJ).

Cell culture and viability

Primary cultures of brain tumor cells were obtained from biopsies donated by the Tumor Bank Network coordinated by the Spanish Cancer Research Centre. HG1 was carried by a 38-year-old man, and HG2 was carried by a 51-year-old man; both were diagnosed by the Pathology Department of Hospital Ramón y Cajal (Madrid, Spain). Tumor samples were homogenized, digested with type Ia collagenase (Sigma) for 1 hr, and incubated on ice for 10 min. The supernatant was collected and, after centrifugation to discard the remaining death-floating cells, resuspended in DMEM containing 15% FBS. Finally,

cells were seeded at a density of 400,000 cells/cm^2 and kept in culture for 2 weeks in DMEM containing 15% FBS and 1% glutamine. Cortical astrocytes were prepared from 24-hr-old Wistar rats as previously described (Gomez del Pulgar et al., 2002b; see also Supplemental Data). C6.9 and C6.4 cells were cultured as described (Galve-Roperh et al., 2000). U87MG, Gos3, MiaPaCa2, A375, and $p8^{+/+}$ and $p8$-deficient Ras^{V12}/E1A-transformed MEFs were cultured in DMEM containing 10% FBS as described (Vasseur et al., 2002a). Cells were transferred to a serum-free medium (except primary cultures of brain tumor cells, A375 cells, and Ras^{V12}/E1A-transformed MEFs, which were transferred to media containing 0.5%, 0.1%, and a 2% FBS, respectively) 18 hr before the different treatments were performed. Cell viability was determined with the CellTiter96 Aqueous One Solution Reagent (MTS) (Promega, Madison, Wisconsin).

Caspase 3/7 activity

Caspase 3/7 (DVEDase) activity was determined using a luminogenic substrate (Caspase Glo, Promega).

Analysis of mitochondrial transmembrane potential

Cells (approximately 0.5×10^6 cells per assay) were trypsinized, collected by centrifugation, washed once, and incubated for 30 min at room temperature with 0.25 μM tetramethylrhodamine methyl ester (TMRM) (Molecular Probes, Leiden, The Netherlands). After incubation for an additional minute with 1 μM Hoechst 33258 (Molecular Probes), fluorescence intensity was analyzed using a LSR flow cytometer (Becton Dickinson, San Jose, CA). Ten thousand cells were recorded in each analysis.

Western blot

Western blot analysis was performed as described (Gomez del Pulgar et al., 2002b). Anti-p8 antibody (Abcam, Cambridge, UK), anti-HA monoclonal antibody (Roche, Basel, Switzerland), and anti-Flag monoclonal antibody (Sigma) were used.

Analysis of gene expression in C6.9 and C6.4 cells

Total RNA was isolated from control and THC-treated C6.9 and C6.4 cells, amplified, labeled, and hybridized on a 22k rat array (Agilent Technologies) (see MIAME in the Supplemental Data).

Analysis of gene expression in rat astrocytes

Total RNA was isolated from vehicle and THC-treated rat primary astrocytes, amplified, labeled, and hybridized on a 22k rat array (Agilent Technologies) (see MIAME in the Supplemental Data).

Analysis of gene expression in *p8*-deficient MEFs

MEFs from *p8* knockout mice immortalized with ras^{V12}/E1A were infected with an empty or a p8-overexpressing retroviral vector as described (Vasseur et al., 2002a). Total RNA was isolated, subsequently amplified, labeled, and hybridized to the GeneChip Mouse Expression Array 430A (Affymetrix, Santa Clara, California) (see MIAME in the Supplemental Data).

Transfections

U87MG cells (75% confluent) were transfected with siRNA duplexes using the X-tremeGENE siRNA Transfection Reagent (Roche) or with a Flag-Bcl-x$_L$-expressing plasmid using Lipofectamine 2000 (Invitrogen). Twenty-four hours after transfection, cells were trypsinized and seeded at a density of 5000 cells/cm^2. Cells were transferred to a serum-free medium 18 hr before performing the different treatments. Transfection efficiency was >70% as monitored by using a control fluorescent siRNA (Qiagen, Hilden, Germany) or a GFP-expressing plasmid.

Infections with p8 retroviral vector

C6.4 cells (75% confluent) were infected with an empty or a p8-overexpressing retroviral vector as described (Vasseur et al., 2002a). Control and p8-overexpressing C6.4 cells were isolated by selection in puromycin (4.5 μg/ml).

Infections with TRB3 adenoviral vector

C6.4 cells (75% confluent) were infected for 1 hr with supernatants obtained from HEK293 cells transduced with adenoviral vectors carrying EGFP or a hemagglutinin-tagged form of rat TRB3 (Iynedjian, 2005). Infection efficiency was >80% as determined by EGFP fluorescence.

RNA interference

Double-stranded RNA duplexes corresponding to human p8 (5′-GGAG GACCCAGGACAGGAU-3′), human ATF-4 (5′-GCCUAGGUCUCUUAGAU GA-3′), human TRB3 (5′-UCAUCUAAGAGAACCUAGGC-3′), human GCS (5′-CCAGGAUAUGAAGUUGCAA-3′), and a nontargeted control (5′-UU CUCCGAACGUGUCACGU-3′) were purchased from Eurogentec (Liege, Belgium).

Reverse transcription-PCR analysis

RNA was isolated with the RNeasy Protect kit (Qiagen). This procedure included a subsequent DNase digestion step using the RNase-free DNase kit (Qiagen). cDNA was obtained with Transcriptor (Roche). Primers were used to amplify mRNA for human p8 (5′-GAAGAGAGGCAGGGAAGACA-3′ and 5′-CTGCCGTGCGTGTCTATTTA-3′ [571 bp product]), human TRB3 (5′-GCCACTGCCTCCCGTCTTG-3′ and 5′-GCTGCCTTGCCCGAGTAT GA-3′ [538 bp product]), human ATF-4 (5′-AGTCGGGGTTTGGGGGCTG

AAG-3′ and 5′-TGGGGAAAGGGGAAGAGGTTGTAA-3′ [436 bp product]), human CHOP (5′-GCGTCTAGAATGGCAGCTGAGTCATTGCC-3′ and 5′-G CGTCTAGATCATGCTTGGTGCAGATTC-3′ [508 bp product]), human GCS (5′-CCTTTCCTCTCCCCACCTTCCTCT-3′ and 5′-GGTTTCAGAAGAGAGA CACCTGGG-3′ [300 bp product]), mouse p8 (5′-GAAGCTGCTGCCAATAC CAACC-3′ and 5′-TAGCTCTGCCCGTCTACCCTC-3′ [359 bp product]), mouse ATF-4 (5′-GAAACCTCATGGGTTCTCCA-3′ and 5′-AGAGCTCATCT GGCATGGTT-3′ [202 bp product]), mouse CHOP (5′-GCAGCCATGGCA GCTGAGTCCCTGCCTTCC-3′ and 5′-CAGACTCGAGGTGATGCCCACTGT TCATGC-3′ [536 bp product]), mouse TRB3 (5′-GCTGGGCTCTCGGCTCC TTTACAT-3′ and 5′-GAGGATTCCCAGGGCCACAAGTCG-3′ [487 bp product]) human/mouse GAPDH (5′-GGGAAGCTCACTGGCATGGCCTTCC-3′ and 5′-CATGTGGGCCATGAGGTCCACCAC-3′ [322 bp product]). PCR reactions were performed using the following parameters: 95ºC for 5 min, 94ºC for 30 s, 57ºC (p8, ATF-4, CHOP, GCS, mTRB3, and GAPDH) or 52ºC (hTRB3) for 30 s, and 72ºC for 1 min, followed by a final extension step at 72ºC for 5 min. The number of cycles was adjusted to allow detection in the linear range.

Real-time quantitative PCR

cDNA was obtained with Transcriptor (Roche). Taqman probes were obtained from Applied Biosystems (Foster City, California). Amplifications were run in a 7700 Real-Time PCR System (Applied Biosystems). Each value was adjusted by using 18S RNA levels as reference.

Ceramide levels

Ceramide levels were determined as previously described (Gomez del Pulgar et al., 2002a).

Metabolic labeling of complex sphingolipids

U87MG cells were incubated with $[^{14}C]$serine (6 μCi/10^6 cells) for 24 hr in serum-free medium before the different treatments were performed. After incubation with either vehicle or THC for 24 additional hr in the same medium, cells were harvested; lipids were extracted with chloroform/methanol and subjected to phase partition with PBS/water. The upper phase was isolated, and ganglioside content was analyzed by thin layer chromatography (TLC) using chloroform/methanol/0.22% $CaCl_2$ (55:45:10, by vol.). The lower phase (containing all non-ganglioside lipids) was subjected to a mild alkaline methanolysis procedure and separated by TLC using chloroform/methanol/ammonia/water (70:30:2:2.5, by vol.).

In vivo treatments

Tumors were induced in nude mice by subcutaneous injection of 10 × 10^6 U87MG cells in PBS supplemented with 0.1% glucose or 10 × 10^6 $p8^{+/+}$ or $p8$-deficient Ras^{V12}/E1A-transformed MEFs in DMEM containing 10% FBS. Tumors were left to grow until they reached an average volume of 200–250 mm^3 (which for U87MG cells and transformed MEFs took around 2 weeks and 10 days, respectively, in the conditions used) and animals were assigned randomly to the different groups. At this point, vehicle or THC (15 mg/kg/day) in 100 μl of PBS supplemented with 5 mg/ml defatted and dialyzed BSA was daily administered in a single peritumoral injection. Tumors were measured with external caliper, and volume was calculated as $(4\pi/3) \times (width/2)^2 \times (length/2)$.

Human tumor samples

Tumor biopsies were obtained from two of the patients enrolled in an ongoing phase I/II clinical trial at the Neurosurgery Department of Tenerife University Hospital (Spain) aimed at investigating the effect of THC administration on the growth of recurrent glioblastoma multiforme. The patients had failed standard therapy, which included surgery, radiotherapy (60 Gy), and temozolamide chemotherapy (2 cycles); had clear evidence of tumor progression on sequential magnetic resonance scanning before enrollment in the study; had received no anticancer therapy for ~6 months; and had a fair health status (Karnofski performance score = 90). The patients provided written informed consent. The protocol was approved by the Clinical Trials Committee of Tenerife University Hospital and by the Spanish Ministry of Health.

The recurrent tumors (Figure S5) were extensively removed by surgery, biopsies were taken, and the tip (~5 cm) of a silastic infusion catheter (9.6 French; 3.2 mm diameter) was placed into the resection cavity. The infusion catheter was connected to a Nuport subclavicular subcutaneous reservoir.

Each day, 0.5–1.5 (median 1.0) mg THC (100 μg/μl in ethanol solution) was dissolved in 30 ml physiological saline solution supplemented with 0.5% (w/v) human serum albumin, and the resulting solution was filtered and administered at a rate of 0.3 ml/min with a syringe pump connected to the subcutaneous reservoir. Patient 1 started the treatment 4 days after the surgery and received THC for 19 days. The posttreatment biopsy was taken 19 days after the cessation of THC administration. Patient 2 started the treatment 4 days after the surgery and received THC for 16 days. The posttreatment biopsy was taken 43 days after the cessation of THC administration. Samples were fixed in formalin and embedded in paraffin.

Immunohistochemistry and TUNEL

Samples from tumor xenografts were dissected and frozen. Samples from human tumors were fixed in 10% buffered formalin and then paraffin embedded. After deparaffinization (only for human tumor samples) and blocking of nonspecific binding, sections were incubated with an anti-human active-caspase 3 antibody (1:200; Promega, Madison, Wisconsin) or with an anti-human p8 antibody (1:500; Vasseur et al., 1999). Immunoperoxidase procedure was performed on xenograft samples using a Vectastain goat anti-rabbit kit (Vector Laboratories, Burlingame, California) and on human tissue using the Ventana gene II device with Ventana kits (Ventana, Strasbourg, France). For TUNEL, samples were labeled with in situ cell death detection kit (Roche). Caspase 3 labeling surface was quantified by an Olympus BX61 automated microscope (10× objective) using Samba 2050 image analyzer (Samba Technologies, Meylan, France).

Statistics

Results shown represent means ± SD. Statistical analysis was performed by ANOVA with a post hoc analysis by the Student-Neuman-Keuls test.

Supplemental data

The Supplemental Data include Supplemental Experimental Procedures and five supplemental figures and can be found with this article online at http://www.cancercell.org/cgi/content/full/9/4/301/DC1/.

References

Benali-Furet, N.L., Chami, M., Houel, L., De Giorgi, F., Vernejoul, F., Lagorce, D., Buscail, L., Bartenschlager, R., Ichas, F., Rizzuto, R., et al. (2005). Hepatitis C virus core triggers apoptosis in liver cells by inducing ER stress and ER calcium depletion. Oncogene *24*, 4921–4933.

Blazquez, C., Casanova, M.L., Planas, A., Gómez del Pulgar, T., Villanueva, C., Fernandez-Acenero, M.J., Aragones, J., Huffman, J.W., Jorcano, J.L., and Guzman, M. (2003). Inhibition of tumor angiogenesis by cannabinoids. FASEB J. *17*, 529–531.

Blazquez, C., Gonzalez-Feria, L., Alvarez, L., Haro, A., Casanova, M.L., and Guzman, M. (2004). Cannabinoids inhibit the vascular endothelial growth factor pathway in gliomas. Cancer Res. *64*, 5617–5623.

Casanova, M.L., Blazquez, C., Martinez-Palacio, J., Villanueva, C., Fernandez-Acenero, M.J., Huffman, J.W., Jorcano, J.L., and Guzman, M. (2003). Inhibition of skin tumor growth and angiogenesis in vivo by activation of cannabinoid receptors. J. Clin. Invest. *111*, 43–50.

Devane, W.A., Hanus, L., Breuer, A., Pertwee, R.G., Stevenson, L.A., Griffin, G., Gibson, D., Mandelbaum, A., Etinger, A., and Mechoulam, R. (1992). Isolation and structure of a brain constituent that binds to the cannabinoid receptor. Science *258*, 1946–1949.

Di Marzo, V., Bifulco, M., and De Petrocellis, L. (2004). The endocannabinoid system and its therapeutic exploitation. Nat. Rev. Drug Discov. *3*, 771–784.

Emberley, E.D., Niu, Y., Curtis, L., Troup, S., Mandal, S.K., Myers, J.N., Gibson, S.B., Murphy, L.C., and Watson, P.H. (2005). The S100A7-c-Jun activation domain binding protein 1 pathway enhances prosurvival pathways in breast cancer. Cancer Res. *65*, 5696–5702.

Galve-Roperh, I., Sanchez, C., Cortes, M.L., Gómez del Pulgar, T., Izquierdo, M., and Guzman, M. (2000). Anti-tumoral action of cannabinoids: involvement of sustained ceramide accumulation and extracellular signal-regulated kinase activation. Nat. Med. *6*, 313–319.

Gaoni, Y., and Mechoulam, R. (1964). Isolation, structure and partial synthesis of an active constituent of hashish. J. Am. Chem. Soc. *86*, 1646–1647.

Garcia-Montero, A.C., Vasseur, S., Giono, L.E., Canepa, E., Moreno, S., Dagorn, J.C., and Iovanna, J.L. (2001). Transforming growth factor β-1 enhances Smad transcriptional activity through activation of p8 gene expression. Biochem. J. *357*, 249–253.

Gomez del Pulgar, T., Velasco, G., Sanchez, C., Haro, A., and Guzman, M. (2002a). De novo-synthesized ceramide is involved in cannabinoid-induced apoptosis. Biochem. J. *363*, 183–188.

Gomez del Pulgar, T., De Ceballos, M.L., Guzman, M., and Velasco, G. (2002b). Cannabinoids protect astrocytes from ceramide-induced apoptosis through the phosphatidylinositol 3-kinase/protein kinase B pathway. J. Biol. Chem. *277*, 36527–36533.

Gouaze, V., Liu, Y.Y., Prickett, C.S., Yu, J.Y., Giuliano, A.E., and Cabot, M.C. (2005). Glucosylceramide synthase blockade down-regulates P-glycoprotein and resensitizes multidrug-resistant breast cancer cells to anticancer drugs. Cancer Res. *65*, 3861–3867.

Guzman, M. (2003). Cannabinoids: potential anticancer agents. Nat. Rev. Cancer *3*, 745–755.

Hoffmeister, A., Ropolo, A., Vasseur, S., Mallo, G.V., Bodeker, H., Ritz-Laser, B., Dressler, G.R., Vaccaro, M.I., Dagorn, J.C., Moreno, S., et al. (2002). The HMG-I/Y-related protein p8 binds to p300 and Pax2 trans-activation domain-interacting protein to regulate the trans-activation activity of the Pax2A and Pax2B transcription factors on the glucagon gene promoter. J. Biol. Chem. *277*, 22314–22319.

Howlett, A.C., Barth, F., Bonner, T.I., Cabral, G., Casellas, P., Devane, W.A., Felder, C.C., Herkenham, M., Mackie, K., Martin, B.R., et al. (2002). International Union of Pharmacology. XXVII. Classification of cannabinoid receptors. Pharmacol. Rev. *54*, 161–202.

Ito, Y., Yoshida, H., Motoo, Y., Iovanna, J.L., Nakamura, Y., Kakudo, K., Uruno, T., Takamura, Y., Miya, A., Noguchi, S., et al. (2005). Expression of p8 protein in breast carcinoma; an inverse relationship with apoptosis. Anticancer Res. *25*, 833–837.

Iynedjian, P.B. (2005). Lack of evidence for a role of TRB3/NIPK as an inhibitor of PKB-mediated insulin signalling in primary hepatocytes. Biochem. J. *386*, 113–118.

Jiang, X., Kim, H.E., Shu, H., Zhao, Y., Zhang, H., Kofron, J., Donnelly, J., Burns, D., Ng, S.C., Rosenberg, S., et al. (2003). Distinctive roles of PHAP proteins and prothymosin-α in a death regulatory pathway. Science *299*, 223–226.

Jiang, W.G., Davies, G., and Fodstad, O. (2005a). Com-1/P8 in oestrogen regulated growth of breast cancer cells, the ER-β connection. Biochem. Biophys. Res. Commun. *330*, 253–262.

Jiang, W.G., Watkins, G., Douglas-Jones, A., Mokbel, K., Mansel, R.E., and Fodstad, O. (2005b). Expression of Com-1/P8 in human breast cancer and its relevance to clinical outcome and ER status. Int. J. Cancer *117*, 30–37.

Li, X.D., Lankinen, H., Putkuri, N., Vapalahti, O., and Vaheri, A. (2005). Tula hantavirus triggers pro-apoptotic signals of ER stress in Vero E6 cells. Virology *333*, 180–189.

Ma, Y., and Hendershot, L.M. (2004). The role of the unfolded protein response in tumour development: friend or foe? Nat. Rev. Cancer *4*, 966–977.

Ma, Y., Brewer, J.W., Diehl, J.A., and Hendershot, L.M. (2002). Two distinct stress signaling pathways converge upon the CHOP promoter during the mammalian unfolded protein response. J. Mol. Biol. *318*, 1351–1365.

Malicet, C., Lesavre, N., Vasseur, S., and Iovanna, J.L. (2003). p8 inhibits the growth of human pancreatic cancer cells and its expression is induced through pathways involved in growth inhibition and repressed by factors promoting cell growth. Mol. Cancer *2*, 37.

Mallo, G.V., Fiedler, F., Calvo, E.L., Ortiz, E.M., Vasseur, S., Keim, V., Morisset, J., and Iovanna, J.L. (1997). Cloning and expression of the rat p8 cDNA, a new gene activated in pancreas during the acute phase of pancreatitis, pancreatic development, and regeneration, and which promotes cellular growth. J. Biol. Chem. *272*, 32360–32369.

Mandic, A., Hansson, J., Linder, S., and Shoshan, M.C. (2003). Cisplatin induces endoplasmic reticulum stress and nucleus-independent apoptotic signaling. J. Biol. Chem. *278*, 9100–9106.

Matsuda, L.A., Lolait, S.J., Brownstein, M.J., Young, A.C., and Bonner, T.I. (1990). Structure of a cannabinoid receptor and functional expression of the cloned cDNA. Nature *346*, 561–564.

McKallip, R.J., Lombard, C., Fisher, M., Martin, B.R., Ryu, S., Grant, S., Nagarkatti, P.S., and Nagarkatti, M. (2002). Targeting CB2 cannabinoid receptors as a novel therapy to treat malignant lymphoblastic disease. Blood *100*, 627–634.

Mechoulam, R., Ben-Shabat, S., Hanus, L., Ligumsky, M., Kaminski, N.E., Schatz, A.R., Gopher, A., Almog, S., Martin, B.R., Compton, D.R., et al. (1995). Identification of an endogenous 2-monoglyceride, present in canine gut, that binds to cannabinoid receptors. Biochem. Pharmacol. *50*, 83–90.

Mimeault, M., Pommery, N., Wattez, N., Bailly, C., and Henichart, J.P. (2003). Anti-proliferative and apoptotic effects of anandamide in human prostatic cancer cell lines: implication of epidermal growth factor receptor down-regulation and ceramide production. Prostate *56*, 1–12.

Munro, S., Thomas, K.L., and Abu-Shaar, M. (1993). Molecular characterization of a peripheral receptor for cannabinoids. Nature *365*, 61–65.

Ogretmen, B., and Hannun, Y.A. (2004). Biologically active sphingolipids in cancer pathogenesis and treatment. Nat. Rev. Cancer *4*, 604–616.

Ohoka, N., Yoshii, S., Hattori, T., Onozaki, K., and Hayashi, H. (2005). TRB3, a novel ER stress-inducible gene, is induced via ATF4-CHOP pathway and is involved in cell death. EMBO J. *24*, 1243–1255.

Piomelli, D. (2003). The molecular logic of endocannabinoid signalling. Nat. Rev. Neurosci. *4*, 873–884.

Portella, G., Laezza, C., Laccetti, P., De Petrocellis, L., Di Marzo, V., and Bifulco, M. (2003). Inhibitory effects of cannabinoid CB1 receptor stimulation on tumor growth and metastatic spreading: actions on signals involved in angiogenesis and metastasis. FASEB J. *17*, 1771–1773.

Riboni, L., Campanella, R., Bassi, R., Villani, R., Gaini, S.M., Martinelli-Boneschi, F., Viani, P., and Tettamanti, G. (2002). Ceramide levels are inversely associated with malignant progression of human glial tumors. Glia *39*, 105–113.

Ruiz, L., Miguel, A., and Diaz-Laviada, I. (1999). Δ^9-tetrahydrocannabinol induces apoptosis in human prostate PC-3 cells via a receptor-independent mechanism. FEBS Lett. *458*, 400–404.

Sanchez, C., Galve-Roperh, I., Canova, C., Brachet, P., and Guzman, M. (1998). Δ^9-tetrahydrocannabinol induces apoptosis in C6 glioma cells. FEBS Lett. *436*, 6–10.

Sarfaraz, S., Afaq, F., Adhami, V.M., and Mukhtar, H. (2005). Cannabinoid receptor as a novel target for the treatment of prostate cancer. Cancer Res. *65*, 1635–1641.

Schroder, M., and Kaufman, R.J. (2005). The mammalian unfolded protein response. Annu. Rev. Biochem. *74*, 739–789.

Su, S.B., Motoo, Y., Iovanna, J.L., Berthezene, P., Xie, M.J., Mouri, H., Ohtsubo, K., Matsubara, F., and Sawabu, N. (2001). Overexpression of p8 is inversely correlated with apoptosis in pancreatic cancer. Clin. Cancer Res. *7*, 1320–1324.

Tajiri, S., Oyadomari, S., Yano, S., Morioka, M., Gotoh, T., Hamada, J.I., Ushio, Y., and Mori, M. (2004). Ischemia-induced neuronal cell death is mediated by the endoplasmic reticulum stress pathway involving CHOP. Cell Death Differ. *11*, 403–415.

Tessitore, A., del P Martin, M., Sano, R., Ma, Y., Mann, L., Ingrassia, A., Laywell, E.D., Steindler, D.A., Hendershot, L.M., and d' Azzo, A. (2004). GM1-ganglioside-mediated activation of the unfolded protein response causes neuronal death in a neurodegenerative gangliosidosis. Mol. Cell *15*, 753–766.

Vasseur, S., Vidal Mallo, G., Fiedler, F., Bodeker, H., Canepa, E., Moreno, S., and Iovanna, J.L. (1999). Cloning and expression of the human p8, a nuclear protein with mitogenic activity. Eur. J. Biochem. *259*, 670–675.

Vasseur, S., Hoffmeister, A., Garcia, S., Bagnis, C., Dagorn, J.C., and Iovanna, J.L. (2002a). p8 is critical for tumour development induced by rasV12 mutated protein and E1A oncogene. EMBO Rep. *3*, 165–170.

Vasseur, S., Hoffmeister, A., Garcia-Montero, A., Mallo, G.V., Feil, R., Kuhbandner, S., Dagorn, J.C., and Iovanna, J.L. (2002b). p8-deficient fibroblasts grow more rapidly and are more resistant to adriamycin-induced apoptosis. Oncogene *21*, 1685–1694.

Accession numbers

Accession numbers to ArrayExpress are E-MEXP-575 (C6.9-C6.4), E-MEXP-576 (astrocytes), and E-MEXP-577 (MEFs).